

Squarato–Metal(II) Complexes. 2. Unusual Bonding Mode for a Squarato-Bridged Trinuclear Copper(II) Complex

Ramon Vicente,^{*,†} Joan Cano,^{†,‡,§} Eliseo Ruiz,^{†,§} Salah S. Massoud,^{*,||} and Franz A. Mautner[⊥]

Departament de Química Inorgànica, Universitat de Barcelona, Martí i Franquès 1-11, 08028 Barcelona, Spain, Institució Catalana de Recerca i Estudis Avançats, Institut de Química Teòrica i Computacional, Universitat de Barcelona, Barcelona, Spain, Department of Chemistry, University of Louisiana at Lafayette, P.O. Box 44370, Lafayette, Louisiana 70504, and Institut für Physikalische and Theoretische Chemie, Technische Universität Graz, A-8010 Graz, Austria

Received November 27, 2007

Herein, we report the structural characterization and magnetic properties of the unique squarato-bridged-tricopper(II) complex, $[\text{Cu}_3(\text{pmap})_3(\mu_{1,2,3}\text{-C}_4\text{O}_4)](\text{ClO}_4)_4 \cdot 2\text{H}_2\text{O}$ (**1**), based on the tripod tripyridylamine ligand bis[2-(2-pyridyl)ethyl]-(2-pyridyl)methylamine (pmap). Each of the three copper centers is penta-coordinated by four N atoms of a pmap ligand and one bridging O atom of the central squarato dianion. This complex is the first example of a non-polymeric X-ray structurally characterized trimeric transition metal complex with the three metal cations being bridged by a single squarato ligand in a $\mu_{1,2,3}$ coordination mode. The magnetic properties of the complex were measured over the temperature range 2–300 K. The complex exhibits moderate bulk antiferromagnetic interaction. The three magnetic exchange pathways have J values of -27.8 , -20.8 , and -31.9 cm^{-1} . The DFT calculations corroborate the relatively strong antiferromagnetic couplings obtained from the fitting of the experimental magnetic susceptibility data and allow an assignment of the fitted J values. Several geometrical parameters have been analyzed using theoretical calculations to establish magnetostructural correlations for complex **1**.

Introduction

The cyclic dianion 3,4-dihydroxycyclobut-3-ene-1,2-dionate, $\text{C}_4\text{O}_4^{2-}$ (squarate ion), is a highly symmetrical planar ligand where its four C–O bonds have partial double-bond character due to its π -electron delocalization. Its similarity to the oxalate dianion, $\text{C}_2\text{O}_4^{2-}$, made it an attractive topic for several studies that led to the formation of bridged metal complexes with different extents of nuclearity and dimensionality.^{1–17} For the bridging squarato ligand and for non-polymeric derivatives, three types of coordination modes,

shown in Scheme 1, are known: μ -1,3- (**1a**),^{1–7} μ -1,2- (**1b**),^{1,5,8,10a} and the uncommon μ -1,2,3,4- (**1c**).^{12,13} Depend-

* Authors to whom correspondence should be addressed. Tel.: +34 934039134, fax: +34 93407725, e-mail: ramon.vicente@qi.ub.es (R.V.). Tel.: +01 337-482-5672, fax: +01 337-482-5676, e-mail: ssmassoud@louisiana.edu (S.S.M.).

[†] Universitat de Barcelona.

[‡] Institució Catalana de Recerca i Estudis Avançats.

[§] Universitat de Barcelona.

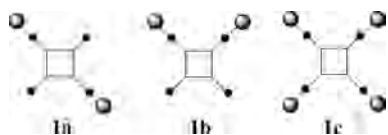
^{||} University of Louisiana at Lafayette.

[⊥] Technische Universität Graz.

- (1) Massoud, S. S.; Mautner, F. A.; Vicente, R.; Dickens, J. S. *Inorg. Chim. Acta* **2008**, *361*, 299.
- (2) Soto, L.; Ruiz, N.; Núñez, H.; Server-Carrió, J.; Escrivà, E.; Sancho, A.; Gracia-Lozano, J. *Inorg. Chim. Acta* **2006**, *359*, 3221.
- (3) Cangussu, D.; Stumpf, H. O.; Adams, H.; Thomas, J. H.; Lloret, F.; Julve, M. *Inorg. Chim. Acta* **2005**, *358*, 2292.

- (4) Kirchmaier, R.; Altin, E.; Lentz, A. Z. *Kristallogr.—New Cryst. Struct.* **2003**, *218*, 541.
- (5) Xanthopoulos, C. E.; Sigalas, M. P.; Katsoulos, G. A.; Tsiapis, C. A.; Hajikostas, C. C.; Terzis, A.; Mentzafos, M. *Inorg. Chem.* **1993**, *32*, 3743.
- (6) Bernardinelli, G.; Deguenon, D.; Soules, R.; Castan, P. *Can. J. Chem.* **1989**, *67*, 1158.
- (7) van Ooijen, J. A. C.; Reedijk, J.; Spek, A. L. *Inorg. Chem.* **1979**, *18*, 1184.
- (8) (a) Krupicka, E.; Lentz, A. Z. *Kristallogr.—New Cryst. Struct.* **2001**, *216*, 287. (b) Krupicka, E.; Lentz, A. Z. *Kristallogr.—New Cryst. Struct.* **2001**, *216*, 289.
- (9) (a) Castro, I.; Calatayud, M. L.; Sletten, J.; Lloret, F.; Julve, M. *J. Chem. Soc., Dalton Trans.* **1997**, 811.
- (10) (a) Castro, I.; Calatayud, M. L.; Sletten, J.; Lloret, F.; Julve, M. *Inorg. Chim. Acta* **1999**, *287*, 173. (b) Zhang, Z.-H.; Yang, H.-L.; Tang, Y.; Ma, Z.-H.; Zhu, Z.-A. *Transition Met. Chem. (Dordrecht, Neth.)* **2004**, *29*, 590. (c) Wang, C.-C.; Yang, C.-H.; Lee, G.-H.; Tsai, H.-L. *Eur. J. Inorg. Chem.* **2005**, 1334.
- (11) Solans, X.; Aguiló, M.; Gleizes, A.; Faus, J.; Julve, M.; Verdager, M. *Inorg. Chem.* **1990**, *29*, 775.
- (12) (a) Akhrif, Y.; Server-Carrió, J.; Sancho, A.; Garcia-Lozano, J.; Escrivà, E.; Soto, L. *Inorg. Chem.* **2001**, *40*, 6832. (b) Hosein, H.-A.; Jaggernauth, H.; Alleyne, B. D.; Hall, L. A.; White, A. J. P.; Williams, D. J. *Inorg. Chem.* **1999**, *38*, 3716.
- (13) Castro, I.; Sletten, J.; Calatayud, M. L.; Julve, M.; Cano, J.; Lloret, F.; Caneschi, A. *Inorg. Chem.* **1995**, *34*, 4903.

Scheme 1



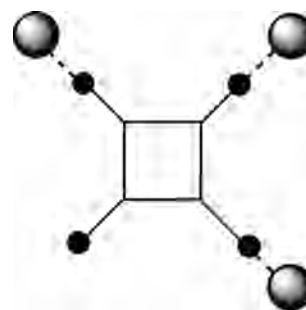
ing on the coordination mode in the squarato-bridged-M^{II} complexes, the intradimer separation distances between the metal centers vary from ca. 5 Å in the cis, μ -1,2- bonding, to 8 Å in the trans, μ -1,3- bonding.^{1–13}

Aqua divalent metal ions tend to form extended polymeric chain structures with the squarato ligand bridging the metal ions in the μ -1,3- coordination mode.¹⁵ Bridged squarato–metal(II) complexes derived from blocking organic ligands afforded dinuclear species with μ -1,3- or μ -1,2-squarato binding; however, polymeric structures *via* μ -1,2- and μ -1,3- coordination have been reported.^{7,15–17} The magnetic measurements on structurally characterized squarato bridged nickel(II) ($|J| = 0.4–1.7 \text{ cm}^{-1}$) and on copper(II) ($|J| = 0–26 \text{ cm}^{-1}$) complexes reveal weak antiferromagnetic interactions between the paramagnetic centers.^{1,9,11} However, weak to very weak ferromagnetic coupling has been also reported.^{3,12,18}

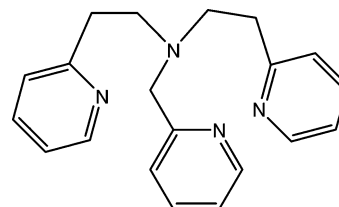
Limiting the discussion on the discrete copper(II) squarato bridged compounds, the dinuclear copper(II) complexes with the μ -1,3-squarato bridging ligand are usually antiferromagnetically coupled with $|J|$ values in the range 0–8.6 cm^{-1} .^{1,10,11} Recently, the compound $[\text{Cu}_2(\text{bpcam})_2(\mu_{1,3}\text{-C}_4\text{O}_4)(\text{H}_2\text{O})_4] \cdot 10\text{H}_2\text{O}$, where bpcam = bis(2-pyrimidylcarbonil)amidate, has been reported to exhibit a weak ferromagnetic interaction ($J = 1.3 \text{ cm}^{-1}$) which has been interpreted on the basis of accidental orthogonality.³ The dinuclear copper(II) complexes with the μ -1,2-squarato bridging ligand show higher $|J|$ values in the range^{1,5,10a} 10.3–26.4 cm^{-1} due to a larger delocalization in the semio-occupied molecular orbitals of μ -1,2-squarato than those of μ -1,3-squarato.⁵ The other described coordination mode is the μ -1,2,3,4.^{12,13} In the full magnetically studied tetranuclear compound $[\text{Cu}_4(\text{tren})_4(\mu_{1,2,3,4}\text{-C}_4\text{O}_4)](\text{ClO}_4)_6$, the fit of the experimental magnetic susceptibilities versus the temperature to the Hamiltonian $H = -J(S_1 \cdot S_2 + S_1 \cdot S_4 + S_2 \cdot S_3 + S_3 \cdot S_4) - j(S_1 \cdot S_3 + S_2 \cdot S_4)$ yields values of -19.0 and -0.8 cm^{-1} for J and j , respectively.¹³

The bonding modes in the non-polymeric squarato bridged copper(II) structures are illustrated in Scheme 1. Inspection of the structurally characterized dinuclear Cu(II) complexes derived from the μ -1,3- (trans), **1a**, and μ -1,2- (cis), **1b**, and from the tetranuclear μ -1,2,3,4-, **1c**, coordination modes led

Scheme 2



Scheme 3



us to predict the existence of trinuclear complexes with the μ -1,2,3- coordination mode (Scheme 2). Therefore, attempts were made to synthesize such complexes, and in the present study, we describe the synthesis, structure, and magnetic characterization of the trinuclear copper(II) compound $[\text{Cu}_3(\text{pmap})_3(\mu_{1,2,3}\text{-C}_4\text{O}_4)](\text{ClO}_4)_4 \cdot 2\text{H}_2\text{O}$ (**1**) based on the ligand bis[2-(2-pyridyl)ethyl]-(2-pyridyl)methylamine (pmap) (see Scheme 3). The complex reveals the trinuclear bonding fashion which is presented in Scheme 2, and as far as we know, the compound represents the first example of a trinuclear compound to be reported with the μ -1,2,3- coordination mode for the squarato ligand. Complex **1** exhibits magnetic properties that are slightly different from those previously reported for squarato Cu^{II} complexes. Hence, we performed a theoretical study using density functional theory methods to assign and corroborate the experimental coupling constants obtained from a fit of the magnetic susceptibility data.

Experimental Section

Materials and Methods. 2-Aminomethylpyridine and 2-vinylpyridine were purchased from Aldrich Chemical Company. 2-vinylpyridine was distilled and purified on silica gel. All other chemicals were reagent-grade-quality. Infrared spectra were recorded on a JASCO FT/IR-480 plus spectrometer as KBr pellets. Electronic spectra were recorded using an Agilent 8453 HP diode UV–vis spectrophotometer. CHN microanalysis was carried out by the Atlantic Microlaboratory, Norcross, Georgia.

Caution! Salts of perchlorate and their metal complexes are potentially explosive and should be handled with great care and in small quantities.

Synthesis of Bis[2-(2-pyridyl)ethyl]-(2-pyridyl)methylamine (pmap). The ligand pmap was prepared and characterized following the procedure described by Karlin's group¹⁹ by refluxing a methanolic solution containing 2-aminomethylpyridine (16.1 g, 0.15 mol), excess freshly distilled 2-vinylpyridine (65 g, 0.62 mol), and

- (14) (a) Graf, M.; Stoeckli-Evans, H.; Escuer, A.; Vicente, R. *Inorg. Chim. Acta* **1997**, *257*, 89. (b) Bencini, A.; Bianchi, A.; Garcia-España, E.; Jeannin, Y.; Julve, M.; Marcelino, V.; Philoche-Levisalles, M. *Inorg. Chem.* **1990**, *29*, 963.
- (15) (a) Lee, C.-R.; Wang, C.-C.; Chen, K.-C.; Lee, G.-H.; Wang, Y. *J. Phys. Chem. A* **1999**, *103*, 156. (b) Alleyne, B. D.; Hall, L. A.; Hosein, H.-A.; Jaggernauth, H.; White, A. J. P.; Williams, D. J. *J. Chem. Soc., Dalton Trans.* **1998**, 3845.
- (16) Soules, R.; Dahan, F.; Laurent, J.-P.; Casten, P. *J. Chem. Soc., Dalton Trans.* **1988**, 587.
- (17) Manna, S. C.; Zangrando, A.; Ribas, J.; Chaudhuri, N. R. *Inorg. Chim. Acta* **2005**, *358*, 4497.
- (18) Mukherjee, P. S.; Konar, S.; Zangrando, E.; Diaz, C.; Ribas, J.; Chaudhuri, P. S. *J. Chem. Soc., Dalton Trans.* **2002**, 3471.

- (19) Schatz, M.; Becker, M.; Thaler, F.; Hampel, F.; Schindler, S.; Jacobson, R. R.; Tyeklár, Z.; Murthy, N. N.; Ghosh, P.; Chen, Q.; Zubieta, J.; Karlin, K. D. *Inorg. Chem.* **2001**, *49*, 2312.

Table 1. Crystallographic Data and Processing Parameters

compound	1
empirical formula	C ₆₄ H ₇₀ Cl ₄ Cu ₃ N ₁₂ O ₂₂
formula mass	1691.77
system	triclinic
space group	<i>P</i> $\bar{1}$
<i>a</i> (Å)	12.554(3)
<i>b</i> (Å)	14.286(3)
<i>c</i> (Å)	21.448(4)
α (deg)	108.93(3)
β (deg)	103.76(3)
γ (deg)	91.86(3)
<i>V</i> (Å ³)	3508.9(12)
<i>Z</i>	2
<i>T</i> (K)	99(2)
μ (Mo K α) (mm ⁻¹)	1.139
<i>D</i> _{calcd} (mg/m ³)	1.601
cryst size (mm)	0.32 × 0.23 × 0.15
θ range (deg)	1.04–25.50
reflns collected	26277
independ. reflns/ <i>R</i> _{int}	12915/0.0463
parameters	1024
goodness-of-fit on <i>F</i> ²	1.178
<i>R</i> 1/ <i>wR</i> 2 (all data)	0.0678/0.1895
residual extrema (<i>e</i> /Å ³)	1.287/–0.689

glacial acetic acid (18 g, 0.30 mol) under nitrogen for 7 days. The compound was purified by charging it onto alumina and eluted by 2% MeOH–ethyl acetate, followed by recrystallization from CH₂Cl₂ using charcoal.

Synthesis of [Cu₃(pmap)₃(μ _{1,2,3}-C₄O₄)](ClO₄)₄·2H₂O. The complex was prepared by the addition of an aqueous solution of disodium squarate (0.045 g, 0.250 mmol) to a preheated aqueous solution containing equimolar amounts of Cu(ClO₄)₂·6H₂O and pmap (0.50 mmol of each/30 mL H₂O). The resulting green solution was heated on a steam bath for 5 min, filtered while hot through celite, and then allowed to crystallize at room temperature. The dark green crystalline compound separated after 2 days and was collected by filtration, washed with 2-propanol and ether, and air-dried (overall yield: 0.240, 85% based on copper(II) perchlorate). Crystals suitable for X-ray crystal structure determination were obtained by crystallization from MeOH. Characterization: Anal. Calcd for C₆₄H₇₀N₁₂Cl₄Cu₃O₂₂ (1691.77 g/mol): C, 45.44; H, 4.17; N, 9.94%. Found: C, 45.14; H, 4.21; N, 9.90%. Selected IR bands (cm⁻¹): ν (O–H) stretching 3435 (m); ν (CO) 1508 (m), 1522 (s), 1489 (s), 1442 (w); ν (Cl–O) (ClO₄⁻) 1089 (vs). Visible spectrum in different solvents { λ _{max}, nm (ϵ _{max}, M⁻¹ cm⁻¹): MeOH, 441, 615 (saturated solution); CH₃CN, 469 (2970), 599 (1280); CH₃NO₂, 458 (2790), 606 (1190); H₂O, 428 (944), 620 (594); DMSO, 470 (2230), 603 (1300).

X-Ray Crystal Structure Analysis. The X-ray single-crystal data were collected on a Bruker-AXS SMART APEX CCD diffractometer with graphite crystal-monochromatized Mo K α radiation ($\lambda = 0.71073$ Å) and processed in a routine manner.^{20–24} Crystallographic data and processing parameters are given in Table 1. The hydrogen atoms were assigned with isotropic displacement

factors and included in the final refinement cycles by use of geometrical constraints. An occupancy of 0.5 was applied to disordered oxygen atoms of perchlorate counterions Cl(3) and Cl(4) and lattice–water molecules O(6) and O(7).

Magnetic Measurements. Magnetic susceptibility measurements for the complex under a magnetic field of 1 T in the range 2–300 K and magnetization measurements in the field range 0–5 T at 2 K were performed with a Quantum Design MPMS-XL SQUID magnetometer at the Magnetochemistry Service of the University of Barcelona. All measurements were performed on polycrystalline samples. Pascal's constants were used to estimate the diamagnetic corrections, which were subtracted from the experimental susceptibilities to give the corrected molar magnetic susceptibilities.

Computational Details. Since a detailed description of the computational strategy used to calculate the exchange coupling constants in polynuclear complexes is outside the scope of this paper, we will only discuss here the most important aspects. A detailed description of the theoretical approach can be found in the literature^{25–28} as well as in a review article for polynuclear complexes.²⁹ For a general polynuclear complex, the Heisenberg Hamiltonian without anisotropic terms can be expressed as

$$\hat{H} = -\sum_{i>j} J_{ij} \hat{S}_i \hat{S}_j \quad (1)$$

where \hat{S}_i and \hat{S}_j are the spin operators of the paramagnetic centers *i* and *j*. The *J*_{*ij*} parameters are the exchange coupling constants for the different pairwise interactions between the paramagnetic metal centers of the molecule. In order to calculate the *n* different coupling constants *J*_{*ij*} present in a polynuclear complex, we need to perform calculations for at least *n* + 1 different spin distributions. By solving the system of *n* equations obtained from the energy differences, we can obtain the *n* coupling constants, and when more than *n* + 1 calculations are performed, then a fitting procedure must be carried out to extract the *J* values. In the case of dinuclear complexes, the *J* value is obtained directly from the energy difference of the high spin state, a triplet state for Cu^{II} complexes, and the broken symmetry solution.^{25,26}

Recently, we have analyzed the effect of the basis set and the choice of the functional on the accuracy of the determination of the exchange coupling constants.^{25,30} The calculations performed using the hybrid B3LYP functional,³¹ together with the basis sets proposed by Schaefer et al., provide *J* values in excellent agreement with the experimental data. We employed a basis set of triple- ζ quality for all atoms.³² The calculations were performed with the Gaussian 03 code³² using initial guess functions generated with the Jaguar 6.0 code.³³

- (20) Blessing, R. H. *Acta Crystallogr.* **1995**, *A51*, 33–38. SADABS; Bruker AXS: Madison, WI, 1998.
- (21) Sheldrick, G. M. *SHELXS-86*, Program for the Solution of Crystal Structure; University of Goettingen: Goettingen, Germany, 1986.
- (22) Sheldrick, G. M. *SHELXL-93*, Program for the Refinement of Crystal Structure; University of Goettingen: Goettingen, Germany, 1993.
- (23) *SHELXTL 5.03* (PC-Version), Program library for the Solution and Molecular Graphics; Siemens Analytical Instruments Division: Madison, WI, 1995.
- (24) ORTEP-3 for Windows; Farrugia, L. J. *J. Appl. Crystallogr.* **1997**, *30*, 565.

- (25) Ruiz, E.; Alvarez, S.; Cano, J.; Polo, V. *J. Chem. Phys.* **2005**, *123*, 164110.
- (26) Ruiz, E.; Cano, J.; Alvarez, S.; Alemany, P. *J. Comput. Chem.* **1999**, *20*, 1391.
- (27) Ruiz, E.; Rodríguez-Forteza, A.; Cano, J.; Alvarez, S.; Alemany, P. *J. Comput. Chem.* **2003**, *24*, 982.
- (28) Ruiz, E.; Alvarez, S.; Rodríguez-Forteza, A.; Alemany, P.; Pouillon, Y.; Massobrio, C. Electronic Structure and Magnetic Behavior in Polynuclear Transition-metal Compounds. In *Magnetism: Molecules to Materials*; Miller, J. S., Drillon, M., Eds.; Wiley-VCH: Weinheim, Germany, 2001; Vol. 2, p 227.
- (29) Ruiz, E. *Struct. Bonding (Berlin)* **2004**, *113*, 71.
- (30) Becke, A. D. *J. Chem. Phys.* **1993**, *98*, 5648.
- (31) Schaefer, A.; Huber, C.; Ahlrichs, R. *J. Chem. Phys.* **1994**, *100*, 5829.

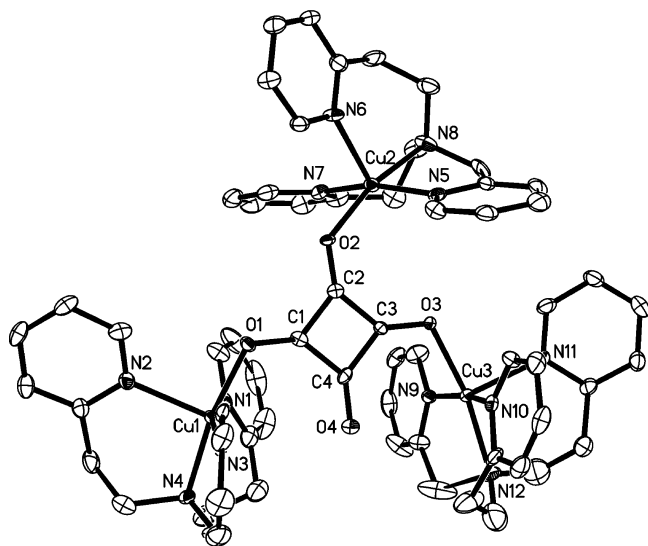


Figure 1. Perspective view of the $[\text{Cu}_3(\text{pmap})_3(\mu_{1,2,3}\text{-C}_4\text{O}_4)]^{4+}$ cation of **1**, together with the atom labeling scheme. The ClO_4^- counterions and lattice water molecules, which are partially disordered, are omitted for clarity.

Results and Discussion

Synthesis of the Complex and Spectroscopic Characterization (See Supporting Information, File S1). Crystal Structure of $[\text{Cu}_3(\text{pmap})_3(\mu_{1,2,3}\text{-C}_4\text{O}_4)](\text{ClO}_4)_4 \cdot 2\text{H}_2\text{O}$ (1**).** A perspective view of the $[\text{Cu}_3(\text{pmap})_3(\mu_{1,2,3}\text{-C}_4\text{O}_4)]^{4+}$ cation of **1**, together with the atom labeling scheme, is given in Figure 1. Main bond parameters are summarized in Table 2. Each of the three copper centers is penta-coordinated by four N atoms of a pmap ligand and one bridging O atom of the central squarato anion. Thus, the squarato anion acts as a $\mu_{1,2,3}$ bridging ligand. The opposite Cu(1) and Cu(3) cations adopt a syn conformation around the squarato ligand (Figures 1 and S2), with a Cu(1)···Cu(3) distance of 6.3300(16) Å; whereas the Cu(1)···Cu(2) and Cu(2)···Cu(3) distances are 6.9289(18) and 5.7156(15) Å, respectively. The coordination polyhedra of the copper(II) centers are very similar, forming distorted square pyramids, with τ values³⁴ of 0.145, 0.057, and 0.053 for Cu(1) to Cu(3), respectively. The Cu centers are shifted from their CuN_3O basal planes by 0.196, 0.192,

and 0.168 Å, respectively. The copper centers Cu(1) and Cu(2) deviate by -0.484 and -0.588 Å, respectively, from the extended plane of the central squarato ligand, whereas Cu(3) lies on this plane [deviation: $+0.040$ Å]. The Cu–O–C bond angles are 118.1(2), 126.4(3), and 113.2(2)°, for Cu(1) to Cu(3), respectively. The Cu–O–C–C torsion angles are 13.1 and 1.8° for Cu1 and Cu3, respectively.

Magnetic Properties. The trinuclear unit in compound **1** exhibits a $\chi_{\text{M}}T$ value of $1.29 \text{ cm}^3 \cdot \text{K} \cdot \text{mol}^{-1}$ at room temperature. This value is similar to that expected for three uncoupled $S = 1/2$ spins ($1.125 \text{ cm}^3 \cdot \text{K} \cdot \text{mol}^{-1}$, $g = 2.0$). With decreasing temperature, $\chi_{\text{M}}T$ decreases, reaching a $0.42 \text{ cm}^3 \cdot \text{K} \cdot \text{mol}^{-1}$ value at 2 K, indicating antiferromagnetic coupling (Figure 2). To understand the magnetic interactions in complex **1**, as a consequence of the different coordination modes and the three different Cu···Cu distances, three coupling parameters (J_{12} , J_{13} , and J_{23}) should be considered (Scheme 4). As a consequence of the scalene triangle coupling scheme, the Hamiltonian to use is $H_1 = -J_1(S_1S_2) - J_2(S_1S_3) - J_3(S_2S_3)$. The fit on the indicated scheme was performed by means of the computer program CLUMAG.³⁵ The best fit parameters were found to be $J_1 = -27.8 \text{ cm}^{-1}$, $J_2 = -20.8 \text{ cm}^{-1}$, $J_3 = -31.9 \text{ cm}^{-1}$, and $g = 2.20$. J_1 , J_2 , or J_3 cannot be assigned directly to one of the coupling parameters J_{12} , J_{13} , or J_{23} . In order to make an assignment, we have performed a theoretical study using density functional methods.

Theoretical Study of the Exchange Interactions. All three of the fitted J values for complex **1** show an unexpected relatively large antiferromagnetic coupling, especially considering that one of them should correspond to the J_{13} interaction, the coupling between the two opposite Cu^{II} cations. The calculated J values using the B3LYP functional (see Computational Details section) are -21.2 , -19.2 , and -25.9 cm^{-1} for J_{12} , J_{13} , and J_{23} interactions, respectively. Such values are reasonably in good agreement with the experimental data taking into consideration the small energy differences involved. Thus, assuming the same order of energies for the calculated and experimental sets of J values, we can assign the fitted J values of -27.8 , -20.8 , and -31.9 cm^{-1} for J_{12} , J_{13} , and J_{23} interactions, respectively. Hence, these results confirm the strength of the interactions obtained experimentally together with the presence of a relatively strong J_{13} value considering a Cu···Cu distance of 6.330 Å. Few examples have been reported of Cu^{II} complexes showing an equivalent J_{13} interaction, and in many of these cases, there is a long Cu–O bond distance with the oxygen atom of the squarato ligand due to the Jahn–Teller effect. Two remarkable examples of copper(II) complexes have been obtained by Castro et al.: the dinuclear $[\text{Cu}_2(\text{bipy})_4(\mu_{1,3}\text{-C}_4\text{O}_4)]^{10a}$ (**2**) and the tetranuclear $[\text{Cu}_4(\text{tren})_4(\mu_{1,2,3,4}\text{-C}_4\text{O}_4)]^{13}$ (**3**) (see Figure 3). The former complex has a structure relatively similar to our complex by considering only the two opposite Cu^{II} cations, whereas the tetranuclear complex **3** corresponds to the situation where all of the oxygen atoms of the squarato bridging ligand are bound to Cu^{II} ions.

(32) Frisch, M. J.; Trucks, G. W.; Schlegel, H. B.; Scuseria, G. E.; Robb, M. A.; Cheeseman, J. R.; Montgomery, J. A.; Vreven, T.; Kudin, K. N.; Burant, J. C.; Millam, J. M.; Iyengar, S. S.; Tomasi, J.; Barone, V.; Mennucci, B.; Cossi, M.; Scalmani, G.; Rega, N.; Petersson, G. A.; Nakatsuji, H.; Hada, M.; Ehara, M.; Toyota, K.; Fukuda, R.; Hasegawa, J.; Ishida, H.; Nakajima, T.; Honda, Y.; Kitao, O.; Nakai, H.; Klene, M.; Li, X.; Knox, J. E.; Hratchian, H. P.; Cross, J. B.; Adamo, C.; Jaramillo, J.; Gomperts, R.; Stratmann, R. E.; Yazyev, O.; Austin, A. J.; Cammi, R.; Pomelli, C.; Ochterski, J.; Ayala, P. Y.; Morokuma, K.; Voth, G. A.; Salvador, P.; Dannenberg, J. J.; Zakrzewski, V. G.; Dapprich, S.; Daniels, A. D.; Strain, M. C.; Farkas, O.; Malick, D. K.; Rabuck, A. D.; Raghavachari, K.; Foresman, J. B.; Ortiz, J. V.; Cui, Q.; Baboul, A. G.; Clifford, S.; Cioslowski, J.; Stefanov, B. B.; Liu, G.; Liashenko, A.; Piskorz, P.; Komaromi, I.; Martin, R. L.; Fox, D. J.; Keith, T.; Al-Laham, M. A.; Peng, C. Y.; Nanayakkara, A.; Challacombe, M.; Gill, P. M. W.; Johnson, B.; Chen, W.; Wong, M. W.; Gonzalez, C.; Pople, J. A. *Gaussian 03*, revision C.1; Gaussian, Inc.: Pittsburgh, PA, 2003.

(33) *Jaguar 6.0*; Schrödinger, Inc.: Portland, OR, 2005.

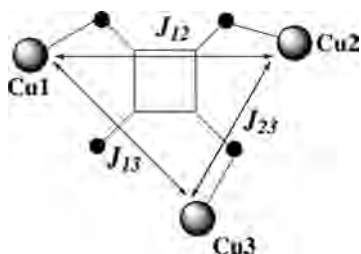
(34) Addison, A. W.; Rao, T. N.; Reedijk, J.; Rijn, J. V.; Verschoor, G. C. *J. Chem. Soc., Dalton Trans.* **1984**, 1349.

(35) The series of calculations were made using the computer program CLUMAG, which uses the irreducible tensor operator formalism (ITO): Gatteschi, D.; Pardi, L. *Gazz. Chim. Ital.* **1993**, *123*, 231.

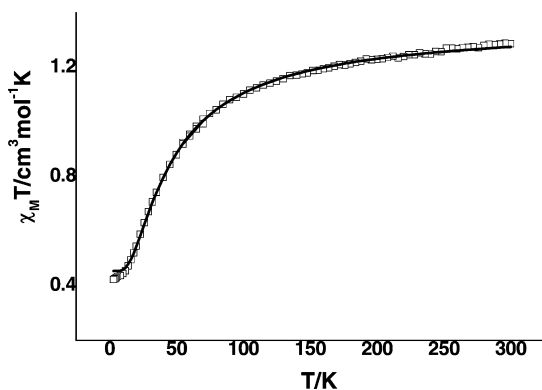
(36) Hay, P. J.; Thibeault, J. C.; Hoffmann, R. *J. Am. Chem. Soc.* **1975**, *97*, 4884.

Table 2. Selected Bond Lengths (Å) and Angles (deg) for **1**

Cu Polyhedra					
Cu(1)–O(1)	1.993(3)	Cu(2)–O(2)	1.962(3)	Cu(3)–O(3)	2.036(2)
Cu(1)–N(3)	2.008(3)	Cu(2)–N(5)	2.000(3)	Cu(3)–N(9)	1.986(3)
Cu(1)–N(1)	2.013(4)	Cu(2)–N(7)	2.001(4)	Cu(3)–N(10)	1.991(4)
Cu(1)–N(4)	2.040(3)	Cu(2)–N(8)	2.044(4)	Cu(3)–N(12)	2.067(4)
Cu(1)–N(2)	2.178(3)	Cu(2)–N(6)	2.187(3)	Cu(3)–N(11)	2.209(3)
Cu(1)···Cu(2)	6.9289(18)	Cu(1)···Cu(3)	6.3300(16)	Cu(2)···Cu(3)	5.7156(15)
O(1)–Cu(1)–N(3)	91.35(12)	O(2)–Cu(2)–N(5)	91.64(12)	N(9)–Cu(3)–O(3)	89.95(12)
O(1)–Cu(1)–N(1)	88.29(12)	O(2)–Cu(2)–N(7)	87.86(13)	N(10)–Cu(3)–O(3)	89.71(12)
N(3)–Cu(1)–N(1)	161.47(12)	N(5)–Cu(2)–N(7)	164.19(13)	N(9)–Cu(3)–N(10)	166.35(13)
O(1)–Cu(1)–N(4)	170.15(11)	O(2)–Cu(2)–N(8)	167.59(11)	O(3)–Cu(3)–N(12)	169.55(13)
N(3)–Cu(1)–N(4)	84.71(14)	N(5)–Cu(2)–N(8)	83.01(14)	N(9)–Cu(3)–N(12)	87.5(2)
N(1)–Cu(1)–N(4)	92.6(2)	N(7)–Cu(2)–N(8)	94.3(2)	N(10)–Cu(3)–N(12)	90.4(2)
O(1)–Cu(1)–N(2)	91.30(11)	O(2)–Cu(2)–N(6)	93.40(12)	N(9)–Cu(3)–N(11)	98.79(13)
N(3)–Cu(1)–N(2)	97.60(13)	N(5)–Cu(2)–N(6)	96.57(13)	N(10)–Cu(3)–N(11)	94.84(13)
N(1)–Cu(1)–N(2)	100.92(13)	N(7)–Cu(2)–N(6)	99.23(13)	O(3)–Cu(3)–N(11)	94.47(11)
N(4)–Cu(1)–N(2)	98.16(13)	N(8)–Cu(2)–N(6)	98.32(13)	N(12)–Cu(3)–N(11)	95.93(13)
Squarato Ligand					
C(1)–O(1)	1.257(4)	C(1)–C(2)	1.467(5)	C(2)–O(2)	1.249(4)
C(2)–C(3)	1.462(5)	C(3)–O(3)	1.267(5)	C(4)–O(4)	1.243(4)
C(1)–C(4)	1.471(5)	C(3)–C(4)	1.463(5)		
O(1)–C(1)–C(2)	133.3(3)	O(3)–C(3)–C(2)	136.5(3)	C(3)–C(4)–C(1)	89.3(3)
O(1)–C(1)–C(4)	136.3(3)	O(3)–C(3)–C(4)	132.6(3)	C(1)–O(1)–Cu(1)	118.1(2)
C(2)–C(1)–C(4)	90.4(3)	C(2)–C(3)–C(4)	90.9(3)	C(2)–O(2)–Cu(2)	126.4(3)
O(2)–C(2)–C(3)	137.7(4)	O(4)–C(4)–C(3)	135.3(3)	C(3)–O(3)–Cu(3)	113.2(2)
O(2)–C(2)–C(1)	132.9(3)	O(4)–C(4)–C(1)	135.4(4)	C(3)–C(2)–C(1)	89.4(3)
C(1)–O(1)–Cu(1)	118.1(2)	C(2)–O(2)–Cu(2)	126.4(3)	C(3)–O(3)–Cu(3)	113.2(2)

Scheme 4. Magnetic Interactions in $[\text{Cu}_3(\text{pmap})_3(\mu_{1,2,3}\text{-C}_4\text{O}_4)(\text{ClO}_4)_4 \cdot 2\text{H}_2\text{O}]$ (**1**)

We have calculated the exchange coupling constant for the dinuclear complex, **2**, shown in Figure 3, obtaining a value of -31 cm^{-1} that is relatively large in comparison with the experimentally fitted value of -8.6 cm^{-1} . The fitted J value for the tetranuclear complex, **3**, from the experimental magnetic susceptibility data is for the first neighbor interaction -19.0 cm^{-1} (equivalent to J_{12} and J_{23} in our complex **1**, see Figure 1), while for the next-nearest neighbor coupling, that is, the interaction between opposite Cu1 and Cu3 cations (this is equivalent to J_{13} in our complex, see Figure 1), it is

**Figure 2.** Temperature dependence of $\chi_{\text{M}}T$ of the solid sample of the complex. Solid line represents the best fit (see text).

-0.8 cm^{-1} .¹³ These values seem to be in contradiction with those obtained experimentally and theoretically for the other two complexes, **1** and **2**, because the J_{13} interaction is considerably weaker in the tetranuclear complex. Thus, in order to verify whether such a small value can be reproduced using the employed theoretical approach, we calculated such interactions assuming that all first neighbor couplings are equivalent, obtaining -9.26 cm^{-1} and -2.0 cm^{-1} for the first neighbor and next-nearest neighbor interactions, respectively. Despite the situation that the first neighbor interaction is weaker than the experimental value, clearly the next-nearest neighbor coupling, which is weaker than that observed in **1**, is in agreement with the experimental data.

Another interesting dinuclear complex, mentioned in the introduction, that shows curious magnetic behavior is $[\text{Cu}_2(\text{bpcam})_2(\text{H}_2\text{O})_4(\mu_{1,3}\text{-C}_4\text{O}_4)]$ (bpcam = bis(2-pyrimidyl)carbonylamidate) (**4**).³ It exhibits ferromagnetic coupling ($J_{13} = +1.3 \text{ cm}^{-1}$) through the squarato bridging ligand (Figure 4). We have calculated the J_{13} value for such a structure obtaining a value of -1.5 cm^{-1} . Despite the disagreement in the sign of the interaction, this complex reveals clearly a smaller antiferromagnetic contribution than that observed in the previous dinuclear complex **2**. Thus, we still have an unanswered question: why is the next-nearest neighbor coupling so strong in complex **1**?

In order to understand how the structural differences between the four complexes might affect the next-nearest neighbor interaction in the studied complexes, we analyzed the structural changes between the four structures: (a) the coordination modes of Cu^{II} cations, (b) the bridging Cu–C–O bond angles, and (c) the Cu–O–C–C torsion angles (see Table 3).

In the trinuclear (**1**) and the two dinuclear complexes (**2** and **4**), the Cu^{II} cations adopt a $4 + 1$ square pyramidal coordination (in Figure 4, one of the water molecules has a

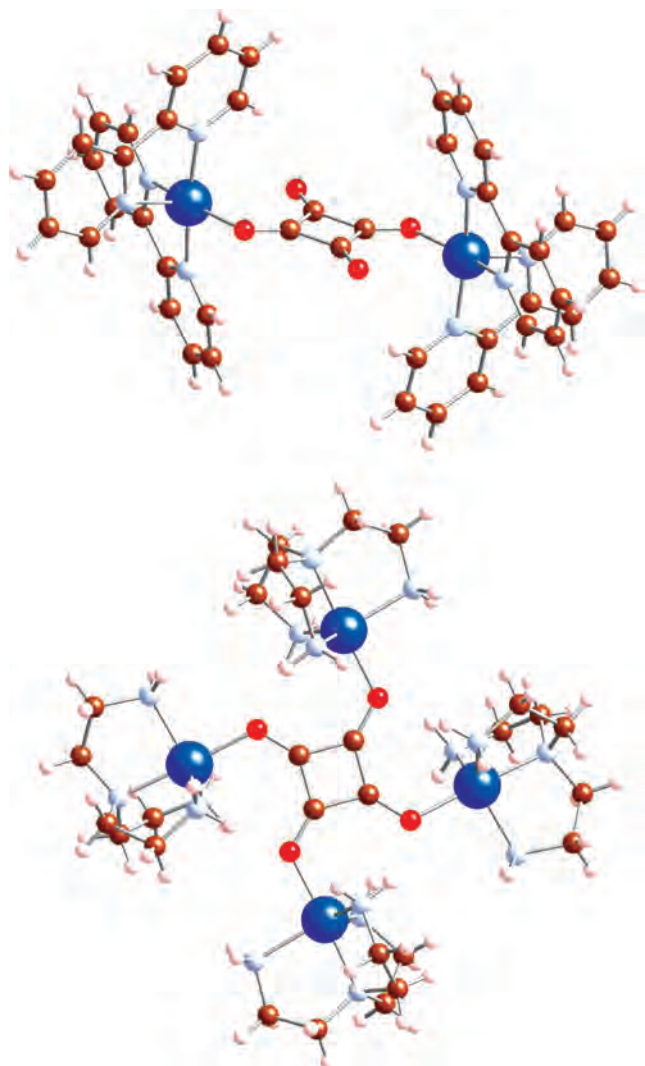


Figure 3. Representation of the bridged squarato complex cations $[\text{Cu}_2(\text{bipy})_4(\mu_{1,3}\text{-C}_4\text{O}_4)]$ (**2**, above) and $[\text{Cu}_4(\text{tren})_4(\mu_{1,2,3,4}\text{-C}_4\text{O}_4)]$ (**3**, below) (charges are omitted for simplicity). Cu^{II} cations are represented by dark blue spheres, while carbon, nitrogen, oxygen, and hydrogen atoms are indicated with brown, light blue, red, and pink spheres, respectively.

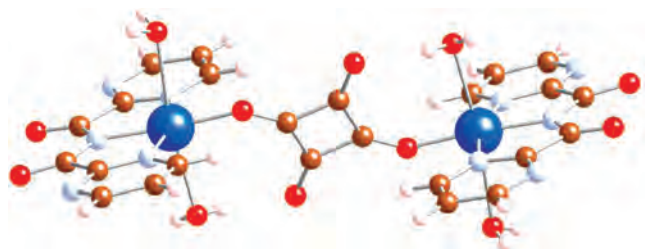


Figure 4. Representation of the dinuclear $[\text{Cu}_2(\text{bpcam})_2(\text{H}_2\text{O})_4(\mu_{1,3}\text{-C}_4\text{O}_4)]$ (**4**) complex (bpcam = bis(2-pyrimidyl)carbonylamidate). Cu^{II} cations are represented by dark blue spheres, while carbon, nitrogen, oxygen, and hydrogen atoms are indicated with brown, light blue, red, and pink spheres, respectively.

very long $\text{Cu}\cdots\text{O}$ distance of 2.609 Å), with the Cu^{II} cation slightly shifted out of the base of the pyramid being the “magnetic orbital”, a $d_{x^2-y^2}$ perpendicular to the squarato plane with one of its lobes oriented toward the oxygen of the squarato ligand. In the tetranuclear complex, **3**, the Cu^{II} centers adopt trigonal bipyramid geometry, and consequently, a d_{z^2} orbital is the “magnetic orbital” (see Figure 5).

Therefore, it should be expected that the interaction in complex **3** occurring through the d_{z^2} orbital should lead to more antiferromagnetic coupling than those observed in the other two complexes (**2** and **4**) due to a larger overlap between magnetic orbitals.¹³ This simple analysis is confirmed by using a model structure with square planar coordination (see Figure 6, syn conformation and $\text{Cu}-\text{O}-\text{C}$ and $\text{Cu}-\text{O}-\text{C}-\text{C}$ angles of 115 and 0°, respectively), obtaining a J_{13} value of -33.9 cm^{-1} , while a distortion in the coordination sphere until reaching a polyhedron close to a trigonal bipyramid enhances the coupling until -43.4 cm^{-1} . Also, the out-of-plane shift of the Cu^{II} cations by 0.2 Å in the square planar coordination increases the antiferromagnetic J_{13} value (-45.9 cm^{-1}). Thus, these two parameters cannot explain the small J_{13} values found experimentally in complexes **2–4**.

We have plotted the results for the previously indicated dinuclear model illustrated in Figure 6 to check the influence of the syn–anti conformations of the squarato bridging ligand and the effect of the $\text{Cu}-\text{O}-\text{C}$ bond angles on the calculated J_{13} values (see Figure 7). The average $\text{Cu}-\text{O}-\text{C}$ angles in the exchange pathway between the opposite Cu^{II} cations are 115.7, 117.0, and 122.1° for the **1–3** complexes, respectively, while the ferromagnetic dinuclear complex (**4**) has a value of 134°. Figure 7 clearly reveals the strong dependence of the J_{13} values on the geometrical conformation. Moreover, the syn conformation, only adopted by complex **1** (see Table 3), produces a slightly stronger antiferromagnetic coupling. For the whole range of $\text{Cu}-\text{O}-\text{C}$ angle values, the coupling is relatively strong and similar to that observed before in the calculated J_{13} values for the dinuclear and trinuclear complexes.

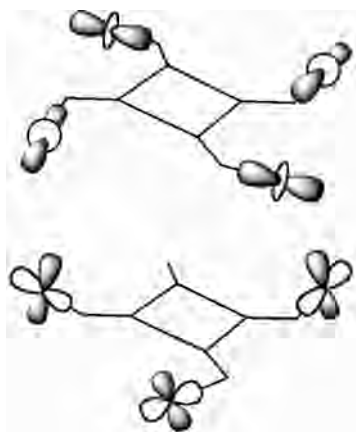
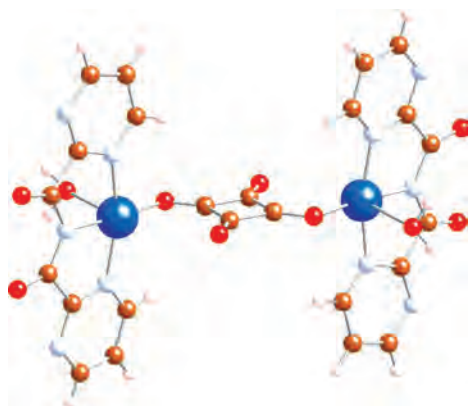
Finally, the last structural difference that we mentioned involves the $\text{Cu}-\text{O}-\text{C}-\text{C}$ torsion angle. Complexes **2** and **3** show relatively small values (see Table 3), while in the asymmetric trinuclear complex, **1**, the $\text{Cu}-\text{O}-\text{C}-\text{C}$ torsion angles are 13.1 and 1.8° for Cu1 and Cu3 , respectively, whereas in the ferromagnetic dinuclear complex **4**, the corresponding value is 13.4°. When the model structure with an anti conformation and a $\text{Cu}-\text{O}-\text{C}$ angle of 135° was used, modifying the structure by changing the $\text{Cu}-\text{O}-\text{C}-\text{C}$ angle from 0 to 13.4° led to a significant decrease of the J_{13} value from -23.2 to -6.0 cm^{-1} . The later distortion seems to be the main factor that reduces considerably the antiferromagnetic contribution in the dinuclear ferromagnetic complex **4** (see Figure 4). This distortion reduces the interaction between the lobes of the $d_{x^2-y^2}$ orbital that is perpendicular to the bridging squarato plane and the π system, resulting in a reduction of the antiferromagnetic term. It is worth mentioning that the analysis of the influence of the asymmetry of the central C_4 axis of the squarato ligand on the J values reveals that the asymmetry of the bond distance found in some complexes induces a negligible change on the exchange coupling constants.

The analysis of the calculated J_{13} values in the studied polynuclear bridged squarato Cu^{II} complexes indicates that the decrease of the number of Cu^{II} cations coordinated to the squarato bridging ligand results in an enhancement of

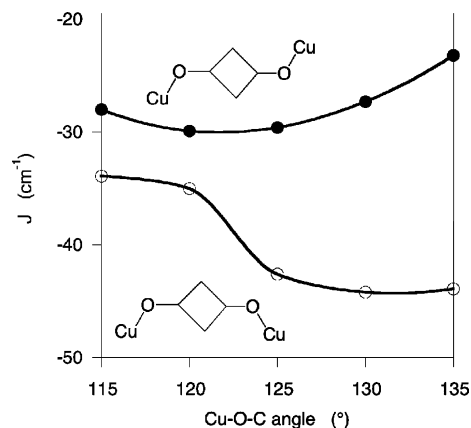
Table 3. Coordination Mode of the Cu^{II} Cations, Square Planar (sp) or Trigonal Bipyramid (tbp) and syn/anti Coordination of the Squarato Ligand in the Four Studied Complexes (1–4)^a

compound			Cu–O–C (deg)	Cu–O–C–C (deg)	exptl. J_{13}	DFT J_{13}
1	[Cu ₃ (pmap) ₃ ($\mu_{1,2,3}$ -C ₄ O ₄)](ClO ₄) ₄	sp, syn	115.7	13.1, 1.8	–20.8	–19.2
2	[Cu ₂ (bipy) ₄ ($\mu_{1,3}$ -C ₄ O ₄)]	sp, anti	117.0	2.3	–8.6	–31
3	[Cu ₄ (tren) ₄ ($\mu_{1,2,3,4}$ -C ₄ O ₄)]	bpt, anti	122.1	7.7	–0.8	–2.0
4	[Cu ₂ (bpcam) ₂ (H ₂ O) ₄ ($\mu_{1,3}$ -C ₄ O ₄)]	sp, anti	134.0	13.4	+1.3	–1.5

^a The more relevant structural data for the magnetostructural correlations and the fitted experimental and calculated J_{13} values are also provided. Average angles are indicated when the corresponding values are similar.

**Figure 5.** Representation of the “magnetic orbitals” corresponding to the tetranuclear (3) and trinuclear (1) studied complexes.**Figure 6.** Representation of the dinuclear model employed in the calculations. Cu^{II} cations are represented by dark blue spheres, while carbon, nitrogen, oxygen, and hydrogen atoms are indicated with brown, light blue, red, and pink spheres, respectively.

the antiferromagnetic contribution for the next-nearest neighbor interaction. Thus, for instance, the calculated J_{13} constant for the tetranuclear complex **3** is -2.0 cm^{-1} , whereas for the trinuclear complex, **1**, it is -19 cm^{-1} . This value is close to that found in model structures where the value of the Cu–O–C–C torsion angle is equal to 0° and the calculated J_{13} values range between -23.2 and -45.9 cm^{-1} (see Figure 7). From such results, we can conclude that the incorporation of the Cu^{II} cations in the 2 and 4 positions of the squarato bridging ligand seems to block or reduce the antiferromagnetic interaction between the two Cu^{II} cations located at the 1 and 3 positions. In order to corroborate such an assumption, we performed calculations of the J_{13} values using again the model structure described in Figure 6 by adding one or two hydrogen atoms in the noncoordinated oxygen atoms of the squarato bridging ligand. This reduces the reference J_{13} value for the original model of -33.9 cm^{-1} to -7.1 and -3.2 cm^{-1}

**Figure 7.** Dependence of the calculated J_{13} value for the dinuclear model (see Figure 6) with the Cu–O–C bond angle for the two conformations of the copper atoms around the squarato ligand. The Cu–O–C–C torsion angles are zero in order to preserve a planar structure.

when one or two hydrogen atoms are added, respectively. We tried to use the Hay–Thibeault–Hoffman model³⁶ to compare the calculated J couplings with the energy gap between the two orbitals bearing the unpaired electrons. However, the analysis of the orbitals bearing the unpaired electrons reveals a large mixture of metal orbitals with those of the ligands, resulting in the presence of more than two orbitals, which shows that this kind of study cannot properly done.

Conclusion

We have synthesized and structurally characterized the squarato-bridged copper(II) trinuclear compound [Cu₃(pmap)₃($\mu_{1,2,3}$ -C₄O₄)](ClO₄)₄·2H₂O (**1**) (pmap = bis[2-(2-pyridyl)ethyl]-(2-pyridyl)methylamine), which shows a new $\mu_{1,2,3}$ coordination mode for the bridged squarato ligand. From the magnetic susceptibility measurements, three fitted J exchange constants of -31.9 , -20.8 , and -27.8 cm^{-1} have been obtained. From theoretical calculations using density functional theory, we can assign these values to the J_{12} , J_{13} , and J_{23} constants, respectively. It is worth noting the relatively large J_{13} value for a next-nearest neighbor coupling. Analysis of the influence of several structural parameters on the J_{13} exchange coupling constant indicates that the syn conformation of the Cu^{II} moieties produces a slightly stronger antiferromagnetic coupling than the equivalent anti conformation, and a relatively more pronounced effect for the Cu–O–C–C torsion angle on this coupling constant. Also, the presence of Cu^{II} cations coordinated in the 2 and 4 positions of the squarato bridging ligand significantly reduces the antiferromagnetic J_{13} exchange coupling constant.

Acknowledgment. This research was partially financially supported by the University of Louisiana at Lafayette, and S.S.M. thanks Dean B. Clark and Dr. R. D. Braun (ULL). F.A.M. thanks Dr. J. Baumgartner (TU-Graz) for assistance. The research reported here was also supported by the Dirección General de Investigación del Ministerio de Educación y Ciencia and Comissió Interdepartamental de Ciència i Tecnologia (CIRIT) through Grants CTQ2005-08123-C02-02/BQU and 2005SGR-00036, respectively. The computing resources were generously made available in the Centre de Supercomputació de Catalunya (CESCA) with a grant

provided by Fundació Catalana per a la Recerca (FCR) and the Universitat de Barcelona. R.V. thanks Ministerio de Educación y Ciencia (CTQ2006-01759).

Supporting Information Available: X-ray crystallographic file in CIF format for compound **1**. The discussion of the synthesis and spectroscopic characterization (S1) and an ORTEP figure (Figure S2) for the complex in TIF format are also included. This material is available free of charge via the Internet at <http://pubs.acs.org>.

IC702324Q